Journal of Medicinal Chemistry

ARTICLE

pubs.acs.org/jmc

Discovery and Optimization of Sulfonyl Acrylonitriles as Selective, Covalent Inhibitors of Protein Phosphatase Methylesterase-1

Daniel A. Bachovchin,[†,§] Andrea M. Zuhl,[†,§] Anna E. Speers,[†] Monique R. Wolfe,[†] Eranthie Weerapana,[†] Steven J. Brown,[‡] Hugh Rosen,[‡] and Benjamin F. Cravatt*[,†]

[†]The Skaggs Institute for Chemical Biology and Department of Chemical Physiology, The Scripps Research Institute, 10550 North Torrey Pines Road, La Jolla, California 92037, United States

[‡]The Scripps Research Institute Molecular Screening Center, The Scripps Research Institute, 10550 North Torrey Pines Road, La Jolla, California 92037, United States

Supporting Information

ABSTRACT: The serine hydrolase protein phosphatase methylesterase-1 (PME-1) regulates the methylesterification state of protein phosphatase 2A (PP2A) and has been implicated in cancer and Alzheimer's disease. We recently reported a fluorescence polarization-activity-based protein profiling (fluopol-ABPP) high-throughput screen for PME-1 that uncovered a remarkably potent and selective class of aza-β-lactam (ABL) PME-1 inhibitors. Here, we describe a distinct set of sulfonyl acrylonitrile inhibitors that also emerged from this screen. The optimized compound, **28** (AMZ30), selectively inactivates PME-1 and reduces the demethylated form of PP2A in living cells. Considering that **28** is structurally unrelated to ABL inhibitors of PME-1, these agents, together, provide a valuable set of pharmacological probes to study the role of methylation in regulating PP2A function. We furthermore observed that several serine hydrolases were sensitive to analogues of **28**, suggesting that more extensive structural exploration of the sulfonyl acrylonitrile chemotype may result in useful inhibitors for other members of this large enzyme class.

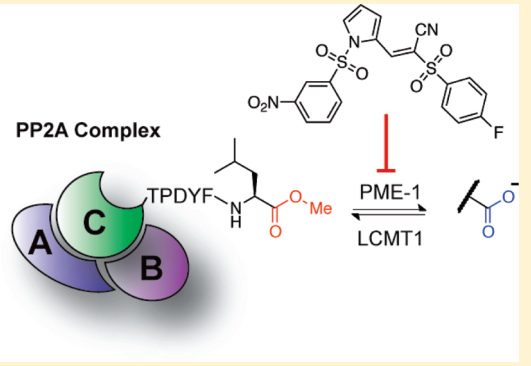

INTRODUCTION

The serine/threonine protein phosphatase 2A (PP2A) is involved in a wide range of cellular processes, including DNA damage repair, cell cycle checkpoint regulation, and the suppression of pro-oncogenic signaling pathways.[1−3] The targeting of PP2A to its many substrates in vivo is critical for proper function and involves dynamic complex assembly with one of several regulatory (B) subunits and posttranslational modifications,[1,2] including C-terminal methylesterification of the catalytic (C) subunit (referred to hereafter as "methylation").[4−7] PP2A methylation is controlled by a methyltransferase (leucine carboxylmethyltransferase-1 or LCMT1)[8] and methylesterase (protein phosphatase methylesterase-1 or PME-1),[9] which install and remove this modification, respectively. The impact of methylation on PP2A function remains largely unknown, but it is thought to modulate B subunit interactions and substrate specificity.[10−13] Studies have implicated reduced PP2A methylation in cancer[14] and neurodegenerative disease,[15] indicating that PME-1 could be an attractive therapeutic target.

Until recently, PME-1 inhibitors had not been reported, possibly because typical substrate assays for PME-1 were incompatible with high-throughput screening (HTS).[16−18] As a serine hydrolase (SH), PME-1 reacts with fluorophosphonate (FP) activity-based probes,[19,20] making it amenable to fluorescence polarization-activity-based protein profiling (fluopol-ABPP), a broadly applicable HTS platform for inhibitor discovery where the ability of compounds to block fluorescent activity-based probe labeling of proteins is monitored by fluorescence polarization.[21] We recently utilized fluopol-ABPP to screen the 300000+ member NIH small-molecule library against PME-1, leading to the discovery of a highly potent (IC_{50} value of ~10 nM) and selective aza-β-lactam PME-1 inhibitor, **1** (Figure 1A; ABL127, NIH Probe ML174).[22,23] Generally speaking, however, it is desirable to generate at least two structurally unrelated classes of inhibitors for an enzyme target like PME-1 because their shared pharmacological activities can then be assigned with confidence to disruption of a common protein target (versus unrelated, compound-specific mechanisms). With this goal in mind, we report here a set of sulfonyl acrylonitrile inhibitors that display high selectivity for PME-1.

RESULTS

HTS by Fluopol-ABPP Identifies a Lead Sulfonyl Acrylonitrile PME-1 Inhibitor. From a 16000 compound Maybridge library screened by fluopol-ABPP, we identified sulfonyl acrylonitrile **2**

Received: April 25, 2011
Published: June 03, 2011

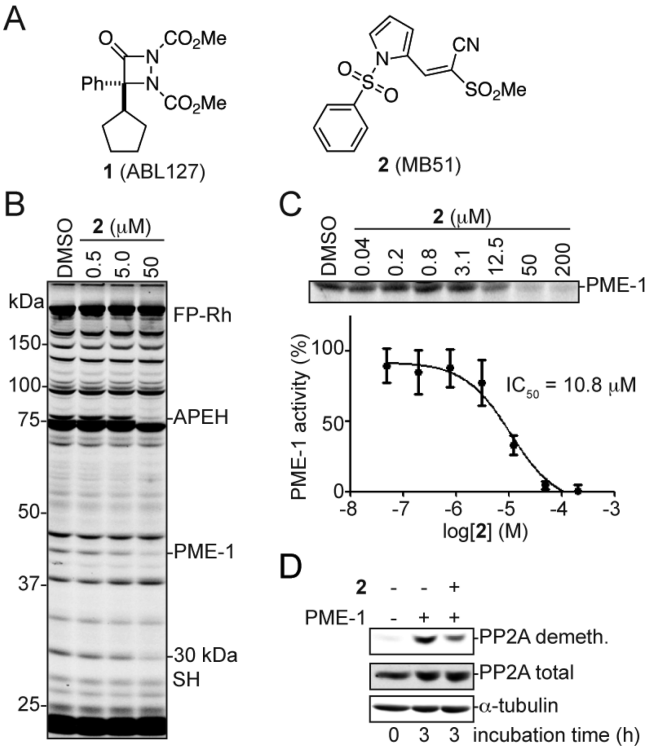

Figure 1. Characterization of lead sulfonyl acrylonitrile PME-1 inhibitor **2**. (A) Structures of **1** and **2**. (B) Evaluation of **2** by gel-based competitive ABPP with FP-Rh (2 μM) in the soluble proteome (1 mg/mL protein) of HEK 293T cells. (C) IC_{50} curve of **2** in the soluble proteome (1 mg/mL protein) from MDA-MB-231 cells as determined by gel-based competitive ABPP (IC_{50} = 10.8 μM). Data are presented as mean values ± SEM; n = 3/group. (D) Pretreatment of HEK 293T proteomes with **2** (50 μM, 10 min) before addition of purified PME-1 (500 nM, 3 h) partially inhibits PP2A demethylation as determined by Western blotting.

(MB51) as a lead PME-1 inhibitor that showed limited off-target activity against other SHs as judged by gel-based competitive ABPP assays[21,24] with an FP-rhodamine (FP-Rh) probe (Figure 1A,B). **2** showed modest potency for PME-1 (IC_{50} = 10.8 μM; Figure 1C) and cross-reacted with two additional SHs in human cell proteomes: acyl-peptide hydrolase (APEH) and an unidentified 30 kDa SH (Figure 1B; Supporting Information Figure S1). Despite its limited potency, **2** (50 μM) partially blocked the PP2A-demethylating activity of PME-1 in cell extracts (Figure 1D). We therefore set out to improve the potency and cellular activity of **2**.

Optimization of the Sulfonyl Acrylonitrile Scaffold for PME-1 Inhibition. We first synthesized a series of analogues with perturbations of the sulfonyl acrylonitrile core of **2** (Table 1), which we suspected might be the key pharmacophore responsible for PME-1 inhibition. We then screened these compounds by competitive ABPP against PME-1 and other SHs in the mouse brain soluble proteome, which contains high levels of the PME-1 protein.[22] We observed that reduction (Scheme 1) of either the olefin (**3**) or the nitrile (**4**) produced inactive compounds. The sulfonamide portion of **2** was also critical for activity as analogues with a free pyrrole group (**7**), a phenyl group (**8**), or an electron-withdrawing *para*-nitrophenyl group (**9**), prepared according to Scheme 2, were all inactive. The presence of mixed electron-withdrawing groups proved important for both activity and

Table 1. Structural Exploration of the Sulfonyl Acrylonitrile Core

Cmpd	Structure	% PME-1 Inhibition (20 μM)	Off-targets[a]
2	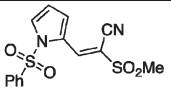	90%	APEH, 30 kDa SH
3	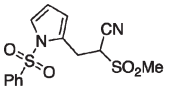	0	-
4	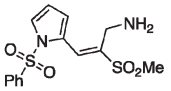	0	-
7	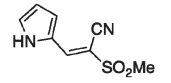	0	-
8	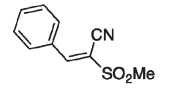	0	-
9	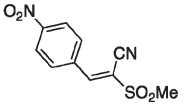	0	-
16	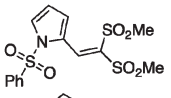	0	PREP
17	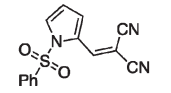	50%	40 kDa SH

[a] Off-targets are defined as SHs with >50% inhibition at 50 μM.

selectivity. For instance, the bis-sulfonyl compound **16** did not inhibit PME-1 but exhibited strong activity against another SH, prolyl endopeptidase (PREP; Supporting Information Figure S2), and the bis-nitrile compound **17** was 2-fold less potent against PME-1 but had increased activity against a 40 kDa SH (Supporting Information Figure S2 and Scheme 3).

We next focused our efforts on modifying the more distal portions of **2**, which led to the discovery that electron-withdrawing groups on the *meta* or *para* positions of the sulfonamide phenyl ring (**18**−**21**) improved potency (Table 2; Supporting Information Figure S3). The addition of these electron-withdrawing groups only increased potency to a point, however, as the strongly electron-withdrawing compound **22** exhibited no activity against PME-1. We next altered the size and electronics of the vinyl sulfone moiety and found that the larger *tert*-butyl (**23**, IC_{50} = 6.8 μM) and electron-withdrawing 4-F-phenyl groups (**25**, IC_{50} = 4.8 μM) improved potency relative to **2**. In addition to showing improved potency, both **23** and **25** were also more selective than **2**, inhibiting only PME-1 in soluble proteomes (Supporting Information Figure S3).

We finally combined the aforementioned features to create **28** (AMZ30; Table 2), a compound that contains 3-NO_2 substituted sulfonamide and 4-F-phenyl sulfonyl groups and showed substantially improved inhibition of PME-1 (IC_{50} value of 600 nM) with more than 100-fold selectivity relative to other SHs in human cell lysates (Figure 2A,B). We believe that **28** (and other acrylonitriles) likely inhibits PME-1 by a covalent, irreversible mechanism because recovery of enzyme activity was not observed

Scheme 1. Reduction of Lead Compound 2[a]

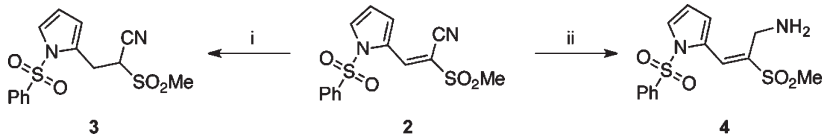

[a] Reagents and conditions: (i) $NaBH_4$, MeOH, 0 °C, 1 h; (ii) LAH, Et_2O, 0 °C, 30 min.

Scheme 2. Synthesis of Compounds 7−14[a]

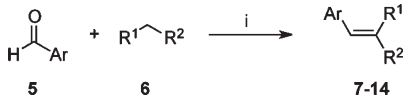

[a] Reagents and conditions: (i) Et_3N, EtOH, mol. sieves, reflux overnight.

Scheme 3. Synthesis of Compounds 6−28[a]

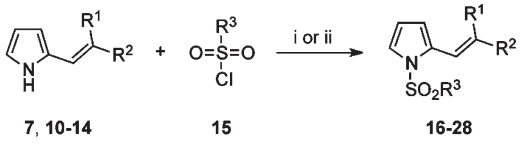

[a] Reagents and conditions: (i) Et_3N; DMF, overnight; (ii) NaH, DMF, 0 °C, overnight.

Table 2. Optimization of the Sulfonyl Acrylonitrile Scaffold for Selective PME-1 Inhibition[a]

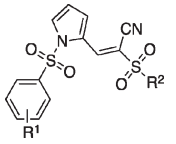

compd	R^1	R^2	PME-1 IC_{50} (μM)	off-targets[b]
18	3-CN	Me	2.5	
19	4-NO_2	Me	3.0	
20	4-Cl	Me	3	APEH
21	4-CN	Me	4	PREP
22	2,3,4,5,6-$(F)_5$	Me	>20	
23	H	*t*-Bu	6.8	
24	H	Ph	>20	
25	H	4-F-Ph	4.8	
26	3-CN	*t*-Bu	3.4	
27	3-CN	4-F-Ph	0.64	
28	3-NO_2	4-F-Ph	0.60	

[a] See Supporting Information Figure S3 for gel-based competitive ABPP data upon which the values in this table are based. [b] Off-targets are defined as SHs with >50% inhibition at 50 μM.

after gel filtration chromatography (Figure 2C). However, we were unable to identify adducts between **28** and the active-site serine nucleophile of PME-1 (or adducts with any other serine or cysteine residue in the protein) by mass spectrometry (MS). We speculate that the putative covalent bond between **28** and PME-1's serine nucleophile, while stable in the context of the folded PME-1 protein, may be broken or eliminated to regenerate the unmodified enzyme following the protein denaturation steps required for MS analysis. While we do not yet know whether the

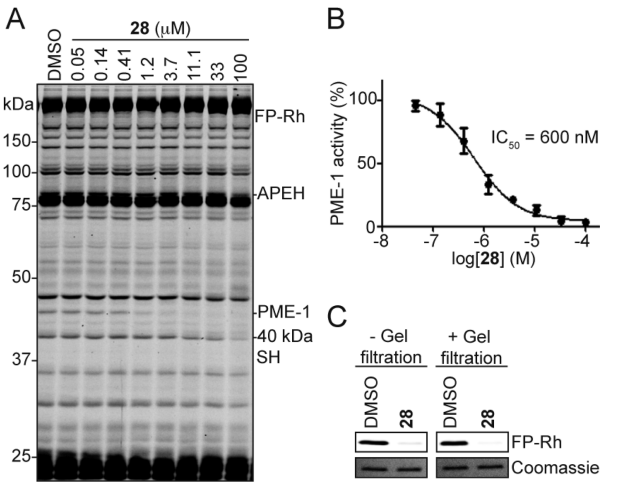

Figure 2. Optimized sulfonyl acrylonitrile **28** selectively inhibits PME-1 in vitro. (A) Evaluation of **28** by gel-based competitive ABPP with FP-Rh (2 μM) in the soluble proteome (1 mg/mL protein) of HEK 293T cells reveals selective PME-1 inhibition with (B) an IC_{50} value of 600 nM. Data are presented as mean values ± SEM; $n = 3$/group. (C) PME-1 (500 nM) was incubated with DMSO or **28** (50 μM), and each reaction was split into two fractions. One fraction was directly labeled with FP-Rh (left panels), and the other was subjected to gel filtration to remove free inhibitor and then reacted with FP-Rh (right panels) to determine the reversibility of inhibition.

olefin or nitrile group in **28** serves as the point of covalent attachment to PME-1, that **16**, which lacks a nitrile group, retains inhibitory activity against other SHs (PREP) leads us to speculate that covalent bond formation through 1,4-Michael addition to the olefin is a likely mechanism for inhibition.

Sulfonyl Acrylonitrile 28 Inhibits PME-1 in Situ. We next asked whether **28** could selectively inhibit PME-1 in living cells. Incubation of HEK 293T cells with a concentration range of **28** generated an in situ IC_{50} value for PME-1 inhibition of 3.5 μM as determined by gel-based ABPP (Figure 3B) without any observed cross-reactivity with other SHs even at 100 μM compound (Figure 3A). We sought to verify the in situ selectivity of **28** by employing the higher resolution, MS-based competitive SILAC-ABPP technology,[22,25] which confirmed complete in situ inhibition of PME-1 and no activity against 35 other SHs detected in HEK 293T cells (Figure 3C). Although these competitive ABPP studies demonstrated that **28** is selective for PME-1 among SHs in HEK 293T cells, they did not address the possibility that **28** interacts with other nucleophilic residues on proteins. Indeed, activated olefins, like the sulfonyl acrylonitriles, have been shown to react with catalytic cysteine and threonine residues in enzymes.[26] To account for this possibility, we incubated soluble proteomes harvested from **28**-treated HEK 293T cells with chloroacetamide-Rh (CA-Rh) or sulfonate ester-Rh (SE-Rh) activity-based probes, which react with activated

dx.doi.org/10.1021/jm200502u | J. Med. Chem. 2011, 54, 5229–5236

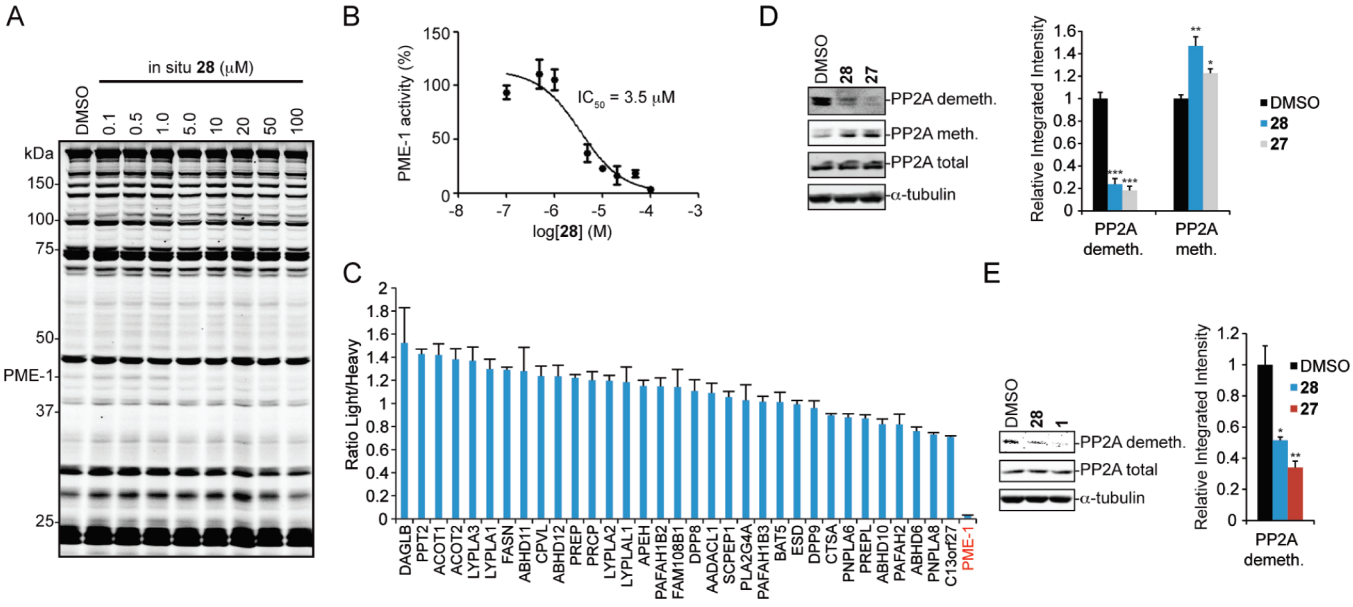

Figure 3. **28** selectively blocks PME-1 activity and reduces levels of demethylated PP2A in cells. (A) Gel-based competitive ABPP with FP-Rh (2 μM) of the soluble proteomes from HEK 293T cells treated with **28** (0.1−100 μM, 1 h) shows selective PME-1 inhibition with (B) an IC_{50} value of 3.5 μM. (C) Isotopically "light" and "heavy" HEK 293T cells were treated with **28** (20 μM) or DMSO, respectively, for 1 h. Proteomes were combined in a 1:1 total protein ratio (0.5 mg each), analyzed by ABPP-MudPIT, and SH activities were quantified by comparing intensities of light and heavy peptide mass peaks. Data are presented as mean values ± SEM for all quantifiable peptides from each SH. (D) HEK 293T cells stably overexpressing PME-1 were treated with **28** or **27** (20 μM, 1 h). Compound-treated cells exhibit significant reductions in demethylated PP2A and significant increases in methylated PP2A, as evident from a representative Western blot (left) and quantified data from replicate experiments (right). (E) Unmodified HEK 293T cells treated with either **28** (20 μM) or **1** (500 nM) for 1 h showed significant reductions in the level of demethylated PP2A. For (D) and (E), $^{*}p < 0.05$, $^{**}p < 0.01$, and $^{***}p < 0.001$ for compound-treated versus DMSO-treated cells. Data are presented as mean values ± SEM; $n = 3$/group.

cysteines and other nucleophilic residues in proteins.[27] **28**, even at 100 μM, did not alter the intensity for any CA-Rh or SE-Rh-labeled proteins relative to their signals in DMSO-treated samples (Supporting Information Figure S4), indicating that **28** is not a generally thiol-reactive compound.

Finally, we investigated the impact of **28** on the methylation state of PP2A. We have shown previously that the effects of PME-1 inhibition are most pronounced in cell lines overexpressing PME-1.[22] Therefore, we initially treated HEK 293T cells stably overexpressing PME-1 with **28** (20 μM) and, for comparison, the structurally related PME-1 inhibitor **27** (20 μM; Table 1), and observed that both inhibitors caused an ~80% reduction in the levels of demethylated PP2A (Figure 3D). **28** and **27** treatment also significantly increased the methylated form of PP2A (Figure 3D). These changes in PP2A methylation state were similar in magnitude to those observed previously with the structurally unrelated inhibitor **1**.[22] **28** (20 μM) and **1** (500 nM) also decreased the demethylated form of PP2A to a similar degree in untransfected HEK 293T cells expressing basal levels of PME-1 (Figure 3E).

CONCLUSIONS

In summary, we have developed a class of sulfonyl acrylonitriles that selectively inhibit the SH PME-1. Essential to the success of this effort were: (1) a fluopol-ABPP HTS assay that enabled the identification of a lead compound with only a modest affinity for PME-1, and (2) the coupling of medicinal chemistry with gel-based competitive ABPP for the parallel refinement of compound potency and selectivity directly in native proteomes. The optimized sulfonyl acrylonitrile compound, **28**, inhibited PME-1 with >100-fold selectivity relative to other SHs in human cells. **28** (designated as NIH Probe ML136), like the previously reported PME-1 inhibitor **1**, significantly reduced the levels of demethylated PP2A and, in cells with elevated levels of PME-1 activity, also increased the levels of methylated PP2A. While **28** is less potent as a PME-1 inhibitor compared to **1**, the fact that these compounds are structurally unrelated should make them useful as paired pharmacological probes to study the role that methylation plays in regulating PP2A function, particularly its impact on determining association with specific B subunits. To this point, it remains possible that **28** and **1** will differentially affect the integrity of PP2A complexes. Indeed, recent crystallographic studies have shown that PME-1 can stably interact with the C subunit of PP2A,[17] and the ABL and sulfonyl acrylonitrile classes of PME-1 inhibitors could affect these protein−protein interactions in different ways.

Projecting forward, we were also intrigued to find that several analogues of **28** inhibit SHs in addition to PME-1, including APEH, PREP, and as-of-yet unidentified 30 kDa and 40 kDa enzymes, in human cell proteomes. These results suggest that further structural exploration of the sulfonyl acrylonitrile class of compounds and, in particular, tuning the electronics of their activated olefin, has the potential to generate selective inhibitors for additional enzymes from the SH class. In this way, the sulfonyl acrylonitrile could take position alongside other classes of covalent SH inhibitors, such as the carbamate,[20,28] lactone/lactam,[22,29] and activated ketones,[24] as a versatile chemotype for expanding our pharmacological coverage of the vast number of SHs present in eukaryotic and prokaryotic organisms.

dx.doi.org/10.1021/jm200502u |J. Med. Chem. 2011, 54, 5229–5236

EXPERIMENTAL SECTION

Synthetic Methods. *Chemistry. General Procedures.* All reactions were carried out in flame-dried glassware under a nitrogen atmosphere with dry solvents, using standard anhydrous techniques. Dry *N*, *N*-dimethylformamide (DMF), methanol (MeOH), and diethyl ether were obtained by passing the previously degassed solvents through activated alumina columns. Absolute ethanol (EtOH) was purchased from Pharmco-AAPER and used without further purification. All reagents were purchased at the highest commercial quality and used without further purification. Reactions were monitored by analytical thin-layer chromatography (TLC) on precoated, glass backed silica gel 60 F_{254} plates. All reported yields are unoptimized. Reactions were purified either by PTLC, also on silica gel 60 F_{254} plates or by flash chromatography on 40−60 MYM mesh silica gel as specified. The purity of tested compounds (>95%) was verified by HPLC using a 12 min gradient elution of increasing concentrations of CH_3CN in water (0−100%) with UV detection at 254 nm on a Gemini C18 50 mm × 4.60 mm, 5 μm column. NMR spectra were recorded on Bruker DRX-600, DRX-500, AMX-400, and Inova-400 instruments and calibrated using residual chloroform as an internal reference. The following abbreviations were used to explain multiplicities: s = singlet, br s = broad singlet, d = doublet, m = multiplet, and all *J* values are reported in Hz. High resolution mass spectra (HRMS) were recorded on an Agilent LC/MSD TOF mass spectrometer by electrospray ionization time-of-flight reflectron experiments. Low resolution mass spectra were recorded on an Agilent LC/MSD ESI mass spectrometer or an Agilent 5973N GC/MS.

*2-(Methylsulfonyl)-3-(1-(phenylsulfonyl)-1H-pyrrol-2-yl)propanenitrile (**3**).* MB51 (5 mg, 0.015 mmol, 1 equiv) was diluted in methanol (150 μL) and cooled to 0 °C under N_2 in a flame-dried half-dram vial. $NaBH_4$ (140 μL, 5 mg/mL in methanol, 1.2 equiv) was then added and the reaction mixture allowed to stir and warm to room temperature over 1 h, at which point it was concentrated in vacuo. PTLC (SiO_2, 250 μm, 70% EtOAc/Hx) afforded 5 mg (0.015 mmol, quant) of the desired product. ^{1}H NMR (400 MHz) δ 7.80−7.78 (m, 2H), 7.68−7.63 (m, 1H), 7.57−7.53 (m, 2H), 7.39−7.38 (m, 1H), 6.39−6.38 (m, 1H), 6.32−6.30 (m, 1H), 4.62 (dd, *J* = 11.4, 4.2, 1H), 3.58 (dd, *J* = 14.6, 4.2, 1H), 3.34 (dd, *J* = 14.6, 11.4, 1H), 3.20 (s,3H). HR-MS *m*/*z* calcd for $C_{14}H_{14}N_2O_4S_2$ (M + Na): 361.0287. Found: 361.0277.

*(E)-2-(Methylsulfonyl)-3-(1-(phenylsulfonyl)-1H-pyrrol-2-yl)prop-2-en-1-amine (**4**).* MB51 (5 mg, 0.015 mmol, 1 equiv) was diluted in ether (150 μL) and cooled to 0 °C under N_2 in a flame-dried half-dram vial. LAH (18 μL, 1 M in THF, 1.2 equiv) was then added slowly dropwise and the reaction mixture allowed to stir for 30 min, at which point it was exposed to air and concentrated under a stream of N_2. PTLC (SiO_2, 250 μm, 80% EtOAc/Hx) afforded 0.6 mg (0.002 mmol, 12%) of the desired product. ^{1}H NMR (500 MHz) δ 7.81−7.79 (m, 2H), 7.64−7.61 (m, 1H), 7.55−7.52 (m, 2H), 7.32−7.31 (m, 1H), 7.26−7.24 (m, 1H), 6.22−6.21 (m, 1H), 6.15−6.14 (m, 1H), 4.29 (s, 2H), 3.76 (s, 2H), 2.58 (s, 3H). HR-MS *m*/*z* calcd for $C_{14}H_{16}N_2O_4S_2$ (M + Na): 363.0444. Found: 363.0448.

General Procedure for the Preparation of Vinyl Aromatics. Powdered 4 Å molecular sieves were charged into a RBF and flame-dried under vacuum. After replacing the atmosphere with nitrogen, ethanol (0.15 M in reactants) was added, followed by the carboxaldehyde (1 equiv), the active methylene compound (1 equiv), and TEA (4 equiv). The reaction was refluxed for 4 h, cooled to room temperature, and then quenched with water (0.5 vol equiv). The aqueous layer was acidified with 1N HCl (0.2 vol equiv) and the product extracted into DCM (3 × 2 vol equiv). The combined organic layers were then washed with water (1 vol equiv), brine (1 vol equiv), dried over $MgSO_4$, and concentrated in vacuo. Flash chromatography (SiO_2, 10−50% EA/Hx gradient) afforded the Knoevenagel products.

*(E)-2-(Methylsulfonyl)-3-(1H-pyrrol-2-yl)acrylonitrile (**7**).* Yield: 18%. ^{1}H NMR (400 MHz) δ 9.64 (br s, 1H), 7.89 (s, 1H), 7.31−7.29 (m, 1H), 7.06−7.02 (m, 1H), 6.50−6.48 (m, 1H), 3.16 (s, 3H). HR-MS *m*/*z* calcd for $C_8H_8N_2O_2S$ (M − H): 195.0234. Found: 195.0240.

*(E)-2-(Methylsulfonyl)-3-phenylacrylonitrile (**8**).* Yield: 43%. ^{1}H NMR (400 MHz) δ 8.14 (s, 1H), 7.96−7.95 (m, 2H), 7.66−7.61 (m, 1H), 7.58−7.53 (m, 2H), 3.22 (s, 3H). ESI-MS *m*/*z* calcd for $C_{10}H_9NO_2S$ (M + H): 208.0. Found: 208.0.

*(E)-2-(Methylsulfonyl)-3-(4-nitrophenyl)acrylonitrile (**9**).* Yield: 13%. ^{1}H NMR (400 MHz) δ 8.41−8.38 (m, 2H), 8.21 (s, 1H), 8.13−8.11 (m, 2H), 3.26 (s, 3H). GC-MS *m*/*z* calcd for $C_{10}H_8N_2O_4S$ (M^+): 252.0. Found: 252.0.

*2-((1H-Pyrrol-2-yl)methylene)malononitrile (**10**).* Yield: 25%. ^{1}H NMR (400 MHz) δ 9.84 (br s, 1H), 7.51 (s, 1H), 7.32−7.30 (m, 1H), 7.05−6.99 (m, 1H), 6.49−6.47 (m, 1H). HR-MS *m*/*z* calcd for $C_8H_5N_3$ (M − H): 142.0411. Found: 142.0415.

*2-(2,2-Bis(methylsulfonyl)vinyl)-1H-pyrrole (**11**).* Yield: 35%. ^{1}H NMR (400 MHz) δ 8.00 (s, 1H), 7.32−7.30 (m, 1H), 6.99−6.97 (m, 1H), 6.45−6.42 (m, 1H), 3.33 (s, 3H), 3.31 (s, 3H). ESI-MS *m*/*z* calcd for $C_8H_{11}NO_4S_2$ (M − H): 249.01. Found: 249.01.

*(E)-2-(Phenylsulfonyl)-3-(1H-pyrrol-2-yl)acrylonitrile (**12**).* Yield: 59%. ^{1}H NMR (400 MHz) δ 9.62 (br s, 1H), 7.99−7.96 (m, 3H), 7.67−7.65 (m, 1H), 7.61−7.56 (m, 2H), 7.24−7.22 (m, 1H), 7.04−7.02 (m, 1H), 6.46−6.44 (m, 1H). ESI-MS *m*/*z* calcd for $C_{13}H_{10}N_2O_2S$ (M − H): 257.0. Found: 257.0.

*(E)-2-((4-Fluorophenyl)sulfonyl)-3-(1H-pyrrol-2-yl)acrylonitrile (**13**).* Yield: 86%. ^{1}H NMR (400 MHz) δ 9.60 (br s, 1H), 8.01−7.97 (m, 2H), 7.96 (s, 1H), 7.28−7.24 (m, 3H), 7.05−7.02 (m, 1H), 6.47−6.45 (m, 1H). ESI-MS *m*/*z* calcd for $C_{13}H_9FN_2O_2S$ (M − H): 275.0. Found: 275.0.

*(E)-2-(tert-Butylsulfonyl)-3-(1H-pyrrol-2-yl)acrylonitrile (**14**).* Yield: 85%.^{1}H NMR (400 MHz) δ 9.90 (br s, 1H), 7.80 (s, 1H), 7.30−7.26 (m, 1H), 7.08−7.05 (m, 1H), 6.48−6.47 (m, 1H), 1.48 (s, 9H). ESI-MS *m*/*z* calcd for $C_{11}H_{14}N_2O_2S$ (M − H): 237.1. Found: 237.0.

General Procedure for the Sulfonation of Pyrroles. To a flame-dried RBF under nitrogen atmosphere was charged the free pyrrole (1 equiv), which was subsequently diluted with DMF (0.05 M in pyrrole). Method A: for the preparation of **19**, **20**, **22**, **23**, **25**, **27**, and **28**, TEA (5 equiv) was then added, followed by the sulfonyl chloride (1.2 equiv). Method B: for the preparaton of **16**−**18**, **21**, **24**, and **26**, the reaction mixture was cooled to 0 °C before the addition of the sulfonyl chloride and then NaH (5 equiv). For both methods A and B, the reactions allowed to stir overnight at which point the solvent was removed in vacuo. PTLC (SiO_2, 1000 mm, 50% EA/Hx) afforded the desired products.

*2-(2,2-Bis(methylsulfonyl)vinyl)-1-(phenylsulfonyl)-1H-pyrrole (**16**).* Yield: 72%. ^{1}H NMR (400 MHz) δ 8.85 (s, 1H), 7.96−7.93 (m, 2H), 7.82−7.81 (m, 1H), 7.74−7.73 (m, 1H), 7.70−7.65 (m, 1H), 7.60−7.55 (m, 2H), 7.52−7.50 (m, 1H), 3.33 (s, 3H), 3.02 (s, 3H). ESI-MS *m*/*z* calcd for $C_{14}H_{15}NO_6S_3$ (M − H): 388.01. Found: 388.01.

*2-((1-(Phenylsulfonyl)-1H-pyrrol-2-yl)methylene)malononitrile (**17**).* Yield: 74%. ^{1}H NMR (400 MHz) δ 8.34 (s, 1H), 7.82−7.79 (m, 2H), 7.76−7.75 (m, 2H), 7.74−7.70 (m, 1H), 7.62−7.58 (m, 2H), 6.58−6.56 (m, 1H). HR-MS *m*/*z* calcd for $C_{14}H_9N_3O_2S$ (M − H): 282.0343. Found: 282.0337.

*(E)-3-(2-(2-Cyano-2-(methylsulfonyl)vinyl)-1H-pyrrol-1-ylsulfonyl) benzonitrile (**18**).* Yield: 6%. ^{1}H NMR (400 MHz) δ 8.63 (s, 1H), 8.15−8.11 (m, 2H), 7.98−7.95 (m, 1H), 7.77−7.74 (m, 3H), 6.55−6.53 (m, 1H), 3.19 (s, 3H). HR-MS *m*/*z* calcd for $C_{15}H_{11}N_3O_4S_2$ (M − H): 360.0118. Found: 360.0130.

*(E)-2-(Methylsulfonyl)-3-(1-((4-nitrophenyl)sulfonyl)-1H-pyrrol-2-yl)acrylonitrile (**19**).* Yield: 34%. ^{1}H NMR (500 MHz) δ 8.65 (s, 1H), 8.43−8.40 (m, 2H), 8.09−8.06 (m, 2H), 7.78−7.75 (m, 2H), 6.64−6.62 (m, 1H), 3.19 (s, 3H). HR-MS *m*/*z* calcd for $C_{14}H_{11}N_3O_6S_2$ (M − H): 380.0011. Found: 380.0023.

*(E)-3-(1-(4-Chlorophenylsulfonyl)-1H-pyrrol-2-yl)-2-(methylsulfonyl)acrylonitrile (**20**).* Yield: 64%. ^{1}H NMR (400 MHz) δ 8.66 (s, 1H), 7.84−7.83 (m, 1H), 7.81−7.80 (m, 1H), 7.75−7.74 (m, 1H), 7.74−7.72 (m, 1H), 7.57−7.56 (m, 1H), 7.55−7.54 (m, 1H), 6.59−6.57 (m, 1H), 3.17 (s, 3H). ESI-MS m/z calcd for $C_{14}H_{11}ClN_2O_4S_2$ (M − H): 369.0. Found: 369.0.

*(E)-4-(2-(2-Cyano-2-(methylsulfonyl)vinyl)-1H-pyrrol-1-ylsulfonyl)benzonitrile (**21**).* Yield: 8%. ^{1}H NMR (400 MHz) δ 8.63 (s, 1H), 8.01−7.98 (m, 2H), 7.90−7.87 (m, 2H), 7.76−7.75 (m, 2H), 6.63−6.61 (m, 1H), 3.19 (s, 3H). HR-MS m/z calcd for $C_{15}H_{11}N_3O_4S_2$ (M − H): 360.0118. Found: 360.0127.

*(E)-2-(Methylsulfonyl)-3-(1-((perfluorophenyl)sulfonyl)-1H-pyrrol-2-yl)acrylonitrile (**22**).* Yield: 31%. ^{1}H NMR (600 MHz) δ 8.62 (s, 1H), 7.83−7.82 (m, 1H), 7.75−7.74 (m, 1H), 6.64−6.63 (m, 1H), 3.18 (s, 1H). ESI-MS m/z calcd for $C_{14}H_7F_5N_2O_4S_2$ (M − H): 425.0. Found: 425.0.

*(E)-2-(tert-Butylsulfonyl)-3-(1-(phenylsulfonyl)-1H-pyrrol-2-yl)acrylonitrile (**23**).* Yield: 45%. ^{1}H NMR (400 MHz) δ 8.59 (s, 1H), 7.90−7.88 (m, 2H), 7.78−7.77 (m, 2H), 7.70−7.67 (m, 1H), 7.60−7.56 (m, 1H), 6.57−6.55 (m, 1H), 1.48 (s, 9H). HR-MS m/z calcd for $C_{17}H_{18}N_2O_4S_2$ (M + Na): 401.0606. Found: 401.0611.

*(E)-2-(Phenylsulfonyl)-3-(1-(phenylsulfonyl)-1H-pyrrol-2-yl)acrylonitrile (**24**).* Yield: 5%. ^{1}H NMR (400 MHz) δ 8.03 (s, 1H), 8.00−7.98 (m, 2H), 7.69−7.66 (m, 3H), 7.62−7.57 (m, 2H), 7.53−7.51 (m, 2H), 7.26−7.24 (m, 1H), 7.11−7.07 (m, 1H), 6.47−6.45 (m, 1H). HR-MS m/z calcd for $C_{19}H_{14}N_2O_4S_2$ (M + Na): 421.0287. Found: 421.0295.

*(E)-2-(4-Fluorophenylsulfonyl)-3-(1-(phenylsulfonyl)-1H-pyrrol-2-yl)acrylonitrile (**25**).* Yield: quantitative. ^{1}H NMR (400 MHz) δ 8.77 (s, 1H), 8.02−7.97 (m, 2H), 7.93−7.92 (m, 1H), 7.91−7.90 (m, 1H), 7.76−7.75 (m, 1H), 7.74−7.70 (m, 1H), 7.63−7.58 (m, 3H), 7.30−7.25 (m, 2H), 6.53−6.51 (m, 1H). HR-MS m/z calcd for $C_{19}H_{13}FN_2O_4S_2$ (M − H): 415.0. Found: 415.0.

*(E)-3-(2-(2-(tert-Butylsulfonyl)-2-cyanovinyl)-1H-pyrrol-1-ylsulfonyl)-benzonitrile (**26**).* Yield: 8%. ^{1}H NMR (400 MHz) δ 8.54 (s, 1H), 8.17−8.14 (m, 1H), 8.12−8.11 (m, 1H), 7.97−7.95 (m, 1H), 7.80−7.74 (m, 3H), 6.64−6.62 (m, 1H), 1.48 (s, 9H). HR-MS m/z calcd for $C_{18}H_{17}N_3O_4S_2$ (M + Na): 426.0553. Found: 426.0568.

*(E)-3-(2-(2-Cyano-2-(4-fluorophenylsulfonyl)vinyl)-1H-pyrrol-1-ylsulfonyl)benzonitrile (**27**).* Yield: 70%. ^{1}H NMR (400 MHz) δ 8.76 (s, 1H), 8.20−8.17 (m, 2H), 8.07−8.03 (m, 2H), 8.02−8.00 (m, 1H), 7.83−7.79 (m, 1H), 7.77−7.75 (m, 1H), 7.69−7.68 (m, 1H), 7.36−7.31 (m, 2H), 6.62−6.60 (m, 1H). HR-MS m/z calcd for $C_{20}H_{12}FN_3O_4S_2$ (M + Na): 464.0145. Found: 464.0152.

*(E)-2-(4-Fluorophenylsulfonyl)-3-(1-(3-nitrophenylsulfonyl)-1H-pyrrol-2-yl)acrylonitrile (**28**).* Yield: 84%. ^{1}H NMR (500 MHz) δ 8.78 (s, 1H), 8.69−8.68 (m, 1H), 8.57−8.55 (m, 1H), 8.28−8.27 (m, 1H), 8.04−8.01 (m, 2H), 7.89−7.86 (m, 1H), 7.77−7.76 (m, 1H), 7.66−7.65 (m, 1H), 7.31−7.28 (m, 2H), 6.60−6.58 (m, 1H). HR-MS m/z calcd for $C_{19}H_{12}FN_3O_6S_2$ (M − H): 400.0079. Found: 400.0096.

Materials for Biological Experiments. FP-biotin,[30,31] FP-rhodamine,[32] SE-rhodamine,[33] and **1**[23] were synthesized following previously described protocols. Demethylated-specific PP2A (clone 4b7), methylated-specific PP2A (clone 2A10), and total PP2A antibodies were purchased from Millipore, anti α-tubulin antibodies were purchased from NeoMarkers, and **2** was purchased from Ryan Scientific. Recombinant PME-1 was expressed and purified as described previously.[22]

Cell Culture and Preparation of Human Cell Line Proteomes. MDA-MB-231 cells were grown in L15 media supplemented with 10% fetal bovine serum at 37 °C in a CO_2 free incubator. HEK 293T cells were grown in DMEM with 10% fetal bovine serum at 37 °C with 5% CO_2. For in vitro experiments, cells were grown to 100% confluency, washed two times with ice cold PBS (pH 7.5), and scraped. Cell pellets were isolated by centrifugation at 1400*g* for 3 min at 4 °C. The pellets were resuspended in 500 μL of ice-cold PBS (pH 7.5), sonicated on ice with a probe sonicator, and centrifuged (64000*g*, 45 min, 4 °C) to provide the soluble fraction as the supernatant and the membrane fraction as the pellet. For in situ experiments, compounds were directly added to the cell culture media and cells incubated at 37 °C for the indicated time before the cells were washed and scraped. The cell pellets were isolated by centrifugation at 1400*g* for 3 min, 4 °C, resuspended in 500 μL of ice-cold PBS (pH 7.5) and sonicated as described above. Then 250 μL of this total cell extract was saved for PP2A methylation analysis by Western blotting (described below), and the remainder was separated into membrane and soluble fractions as described above. PME-1 was stably overexpressed in HEK 293T cells as described previously.[22] Rat APEH and mouse PREP were transiently overexpressed in COS-7 cells as described previously.[20] Total protein concentration of each fraction was determined using a protein assay kit (Bio-Rad). Samples were stored at −80 °C until use.

Competitive ABPP Assays in Proteomes. For in vitro experiments, proteomes were diluted to 1 mg/mL in PBS (pH 7.5) and incubated with DMSO or compound for 30 min at 25 °C (25 μL total reaction volume). FP-rhodamine was then added at a final concentration of 2 μM. After 45 min, the reactions were quenched with 2× SDS-PAGE loading buffer (reducing), separated by SDS-PAGE (10% acrylamide), and visualized in-gel with a Hitachi FMBio IIe flatbed fluorescence scanner (MiraiBio). For in situ experiments, soluble proteomes were prepared from harvested cells treated with DMSO or compound as indicated and diluted to 1 mg/mL in PBS (25 μL total volume). These proteomes were then directly labeled with rhodamine probe as follows: FP-rhodamine (2 μM, 45 min), CA-rhodamine (5 μM, 1 h), or SE-rhodamine (5 μM, 1 h) at 25 °C, and analyzed as described above.

Determination of IC_{50} Values. For determination of in vitro IC_{50} values, compounds were incubated in the indicated soluble proteome (1 mg/mL, 25 μL total volume) at the specified concentrations (performed in triplicate) for 45 min at 37 °C. The samples were then labeled with FP-rhodamine (2 μM) for 45 min, quenched with 2× loading buffer (reducing), separated by SDS-PAGE, and visualized by in-gel fluorescence scanning. For determination of in situ IC_{50} values, the soluble fractions from cells treated with compound (1 h, performed in triplicate using conditions described above) were diluted to 1 mg/mL in PBS (25 μL total volume) and then labeled with FP-rhodamine and analyzed as described above. The percentage activity remaining was determined by measuring the integrated optical intensity of the bands using ImageJ software. IC_{50} values were determined from a dose−response curve generated using Prism software (GraphPad).

Assessing the Reversibility of Inhibition. Purified wild-type PME-1 (500 nM, 2.6 mL total volume in PBS) was incubated with DMSO or **28** (50 μM) at 25 °C. After 30 min, 100 μL was removed from each reaction (fraction A). The remaining 2.5 mL of each reaction was passaged over a Sephadex G-25 M column (GE Healthcare) and eluted in a volume of 3.5 mL PBS (fraction B). Then 100 μL of both fractions A and B were labeled with FP-rhodamine (2 μM, as described above). After 30 min, the reactions were quenched with 2× SDS-PAGE loading buffer, separated by SDS-PAGE, and analyzed by in-gel fluorescence scanning. Gels were then subjected to Coomassie staining with Instant-Blue (Expedeon) to verify equivalent protein loading.

Isotopic Competitive ABPP-MudPIT. HEK 293T cells were grown in DMEM SILAC media (ThermoScientific) supplemented with dialyzed fetal bovine serum (Gemini) and $^{12}C^{14}N$-lysine and -arginine (Sigma) for "light" cells or $^{13}C_6{}^{15}N_2$-lysine and -arginine (Isotec) for "heavy" cells. Cells were treated as indicated with DMSO or **28** (1 h, 37 °C), washed, harvested, and soluble and membrane proteomes were isolated as described above. Light and heavy proteome fractions (0.5 mg each) were combined (1 mL total volume) and labeled with 5 μM of FP-biotin for 1 h at 25 °C. After incubation, the membrane proteomes were solubilized with 1% Triton-X and rotated at 4 °C for 1 h. Enrichment of FP-labeled proteins was achieved as previously described.[34] The

streptavidin-enriched proteome was washed two times for 3 min with (1) 1% SDS in PBS, (2) 6 M urea in PBS, (3) PBS (pH 7.5), and finally resuspended in 200 μL of 8 M urea in 25 mM ammonium bicarbonate. Samples were then prepared for on-bead digestion by reduction with 10 mM TCEP (Sigma) for 30 min at 25 °C and alkylation with 12 mM iodoacetamide (Sigma) for 30 min at 25 °C in the dark. Samples were diluted to 2 M urea with PBS (pH 7.5), and digestions were performed for 12 h at 37 °C with sequence-grade modified trypsin (Promega; 4 μL of 0.5 μg/μL) in the presence of 2 mM $CaCl_2$. Last, peptide samples were acidified with formic acid to a final concentration of 5%.

Digested peptide mixtures were pressure-loaded on a fused silica loading column (250 μm i.d., 360 μm o.d.) packed with 4 cm of reversed-phase resin (Aqua C18, 5 μm, 125A, Phenomenex) fitted with a fritted filter (Upchurch). The loading column was attached in-line to a biphasic MudPIT capillary column (100 μm i.d., 360 μm o.d., packed with 10 cm Aqua C18 reversed phase resin followed by 3 cm strong cation exchange resin (Partisphere, 5 μm, 120A, Whatman) with an in-house pulled tip). The sample was analyzed by two-dimensional liquid chromatography (2D-LC) separation in combination with tandem mass spectrometry as previously described[34,35] using an Agilent 1100-series quaternary pump (manual flow-split system) and LTQ-Orbitrap Velos mass spectrometer running Xcalibur Software (ThermoScientific). The mass spectrometer was outfitted with an in-house fabricated nanospray platform. Peptides were eluted in a five-step MudPIT experiment (using 0%, 10%, 25%, 80%, and 100% salt bumps of 500 mM aqueous ammonium acetate, each step followed by an increasing gradient of aqueous acetonitrile/0.1% formic acid) and data were collected in data-dependent acquisition mode with dynamic exclusion enabled (repeat count of 1, exclusion duration of 20 s). One full MS1 scan (400−1800 m/z) was followed by 30 data dependent MS2 scans of the most abundant ions with monoisotopic precursor selection enabled. All other parameters were left at default values. The MS2 spectra data were extracted from the raw file using RAW Xtractor (version 1.9.7; publically available at http://fields.scripps.edu/?q=content/download). MS2 spectra data were searched using the SEQUEST algorithm (Version 3.0)[36] against the latest version of the human IPI database concatenated with the reversed database for assessment of false-discovery rate.[37] SEQUEST searches allowed for variable oxidation of methionine (+16), static modification of cysteine residues (+57 due to alkylation), and no enzyme specificity. Each data set was independently searched with light and heavy params files: for the light search, all other amino acids were left at default masses; for the heavy search, static modifications on lysine (8.0142) and arginine (10.0082) were specified. The resulting MS2 spectra matches were assembled into protein identifications and filtered using DTASelect (version 2.0.41)[38] with the --trypstat option, which applies different statistical models for the analysis of tryptic, half-tryptic, nontryptic peptides, and peptides were restricted to fully tryptic using the -y 2 option. DTASelect 2.0 uses a quadratic discriminant analysis to achieve a user-defined maximum peptide false positive rate; the default parameters (maximum false positive rate of 5%) was used for the search; however, the actual false positive rate was much lower (<1%). SILAC ratios were quantified using in-house software.[39] The total proteomic data was filtered manually for serine hydrolases containing at least two quantifiable peptides, and data was globally normalized to a control sample where both heavy and light cells were treated with DMSO and mixed in a 1:1 ratio to adjust heavy to light peptide abundance to exactly a 1:1 ratio (correction factor = 1.3 light/heavy). Two serine hydrolases, BCHE and CES3, displayed ratios >3 light:heavy in the control sample that were maintained in the inhibitor-treated sample and, for simplicity, were excluded from analysis.

Immunoblot Analysis. Proteomes (treated as indicated) were diluted to 2 mg/mL in PBS, denatured with standard 2× SDS-PAGE loading buffer (reducing), separated by SDS-PAGE (10% acrylamide), and analyzed by Western blotting using standard methods. Blots were probed using indicated antibodies following manufacturers' instructions and were visualized and quantified using the Odyssey imaging system (Li-Cor).

■ ASSOCIATED CONTENT

Supporting Information. Evaluations of **2** and **16**; representative gel-based competitive ABPP profiles for **18**, **19**, **20**, **21**, **23**, **25**, **26**, **27**, and **28**; selectivity profiling of **28** for cross-reactivity; detailed synthesis of the chloroacetamide (CA)-rhodamine probe. This material is available free of charge via the Internet at http://pubs.acs.org.

■ AUTHOR INFORMATION

Corresponding Author

*Phone: 858-784-8633. E-mail: cravatt@scripps.edu.

Author Contributions

§These authors contributed equally to this work.

■ ACKNOWLEDGMENT

We thank Tianyang Ji, David Milliken, Kim Masuda, and Benjamin Kipper for technical assistance. This work was supported by the National Institutes of Health CA132630 (B.F.C.), MH084512 (B.F.C., H.R.), the National Science Foundation (predoctoral fellowships to D.A.B. and A.M.Z.), the California Breast Cancer Research Program (predoctoral fellowship to D.A.B.), and The Skaggs Institute for Chemical Biology.

■ ABBREVIATIONS USED

PP2A, protein phosphatase 2A; PME-1, protein phosphatase methylesterase-1; fluopol, fluorescence polarization; ABPP, activity-based protein profiling; ABL, aza-β-lactam; LCMT1, leucine carboxylmethyltransferase-1; FP, fluorophosphonate; SH, serine hydolase; HTS, high-throughput screening; Rh, rhodamine; APEH, acyl-peptide hydrolase; PREP, prolyl endopeptidase; SILAC, stable isotope labeling with amino acids in cell culture; CA, chloroacetamide; SE, sulfonate ester

■ REFERENCES

(1) Shi, Y. Serine/threonine phosphatases: mechanism through structure. *Cell* **2009**, *139*, 468–484.

(2) Janssens, V.; Goris, J. Protein phosphatase 2A: a highly regulated family of serine/threonine phosphatases implicated in cell growth and signalling. *Biochem. J.* **2001**, *353*, 417–439.

(3) Millward, T. A.; Zolnierowicz, S.; Hemmings, B. A. Regulation of protein kinase cascades by protein phosphatase 2A. *Trends Biochem. Sci.* **1999**, *24*, 186–191.

(4) Chen, J.; Martin, B. L.; Brautigan, D. L. Regulation of protein serine-threonine phosphatase type-2A by tyrosine phosphorylation. *Science* **1992**, *257*, 1261–1264.

(5) Guo, H.; Damuni, Z. Autophosphorylation-activated protein kinase phosphorylates and inactivates protein phosphatase 2A. *Proc. Natl. Acad. Sci. U.S.A* **1993**, *90*, 2500–2504.

(6) Favre, B.; Zolnierowicz, S.; Turowski, P.; Hemmings, B. A. The catalytic subunit of protein phosphatase 2A is carboxyl-methylated in vivo. *J. Biol. Chem.* **1994**, *269*, 16311–16317.

(7) Xie, H.; Clarke, S. An enzymatic activity in bovine brain that catalyzes the reversal of the C-terminal methyl esterification of protein phosphatase 2A. *Biochem. Biophys. Res. Commun.* **1994**, *203*, 1710–1715.

(8) Lee, J.; Stock, J. Protein phosphatase 2A catalytic subunit is methyl-esterified at its carboxyl terminus by a novel methyltransferase. *J. Biol. Chem.* **1993**, *268*, 19192–19195.

(9) Lee, J.; Chen, Y.; Tolstykh, T.; Stock, J. A specific protein carboxyl methylesterase that demethylates phosphoprotein phosphatase 2A in bovine brain. *Proc. Natl. Acad. Sci. U.S.A* **1996**, *93*, 6043–6047.

(10) Tolstykh, T.; Lee, J.; Vafai, S.; Stock, J. B. Carboxyl methylation regulates phosphoprotein phosphatase 2A by controlling the association of regulatory B subunits. *EMBO J.* **2000**, *19*, 5682–5691.

(11) Wu, J.; Tolstykh, T.; Lee, J.; Boyd, K.; Stock, J. B.; Broach, J. R. Carboxyl methylation of the phosphoprotein phosphatase 2A catalytic subunit promotes its functional association with regulatory subunits in vivo. *EMBO J.* **2000**, *19*, 5672–5681.

(12) Bryant, J. C.; Westphal, R. S.; Wadzinski, B. E. Methylated C-terminal leucine residue of PP2A catalytic subunit is important for binding of regulatory Balpha subunit. *Biochem. J.* **1999**, *339*, 241–246.

(13) Longin, S.; Zwaenepoel, K.; Louis, J. V.; Dilworth, S.; Goris, J.; Janssens, V. Selection of protein phosphatase 2A regulatory subunits is mediated by the C terminus of the catalytic Subunit. *J. Biol. Chem.* **2007**, *282*, 26971–26980.

(14) Puustinen, P.; Junttila, M. R.; Vanhatupa, S.; Sablina, A. A.; Hector, M. E.; Teittinen, K.; Raheem, O.; Ketola, K.; Lin, S.; Kast, J.; Haapasalo, H.; Hahn, W. C.; Westermarck, J. PME-1 protects extracellular signal-regulated kinase pathway activity from protein phosphatase 2A-mediated inactivation in human malignant glioma. *Cancer Res.* **2009**, *69*, 2870–2877.

(15) Lee, K. W.; Chen, W.; Junn, E.; Im, J. Y.; Grosso, H.; Sonsalla, P. K.; Feng, X.; Ray, N.; Fernandez, J. R.; Chao, Y.; Masliah, E.; Voronkov, M.; Braithwaite, S. P.; Stock, J. B.; Mouradian, M. M. Enhanced phosphatase activity attenuates alpha-synucleinopathy in a mouse model. *J. Neurosci.* **2011**, *31*, 6963–6971.

(16) Ogris, E.; Du, X.; Nelson, K. C.; Mak, E. K.; Yu, X. X.; Lane, W. S.; Pallas, D. C. A protein phosphatase methylesterase(PME-1) is one of several novel proteins stably associating with two inactive mutants of protein phosphatase 2A. *J. Biol. Chem.* **1999**, *274*, 14382–14391.

(17) Xing, Y.; Li, Z.; Chen, Y.; Stock, J. B.; Jeffrey, P. D.; Shi, Y. Structural mechanism of demethylation and inactivation of protein phosphatase 2A. *Cell* **2008**, *133*, 154–163.

(18) Longin, S.; Jordens, J.; Martens, E.; Stevens, I.; Janssens, V.; Rondelez, E.; De Baere, I.; Derua, R.; Waelkens, E.; Goris, J.; Van Hoof, C. An inactive protein phosphatase 2A population is associated with methylesterase and can be re-activated by the phosphotyrosyl phosphatase activator. *Biochem. J.* **2004**, *380*, 111–119.

(19) Blankman, J. L.; Simon, G. M.; Cravatt, B. F. A comprehensive profile of brain enzymes that hydrolyze the endocannabinoid 2-arachidonoylglycerol. *Chem. Biol.* **2007**, *14*, 1347–1356.

(20) Bachovchin, D. A.; Ji, T.; Li, W.; Simon, G. M.; Blankman, J. L.; Adibekian, A.; Hoover, H.; Niessen, S.; Cravatt, B. F. Superfamily-wide portrait of serine hydrolase inhibition achieved by library-versus-library screening. *Proc. Natl. Acad. Sci. U.S.A* **2010**, *107*, 20941–20946.

(21) Bachovchin, D. A.; Brown, S. J.; Rosen, H.; Cravatt, B. F. Identification of selective inhibitors of uncharacterized enzymes by high-throughput screening with fluorescent activity-based probes. *Nature Biotechnol.* **2009**, *27*, 387–394.

(22) Bachovchin, D. A.; Mohr, J. T.; Speers, A. E.; Wang, C.; Berlin, J. M.; Spicer, T. P.; Fernandez-Vega, V.; Chase, P.; Hodder, P. S.; Schurer, S. C.; Nomura, D. K.; Rosen, H.; Fu, G. C.; Cravatt, B. F. Organic Synthesis Toward Small-Molecule Probes and Drugs Special Feature: Academic Cross-Fertilization by Public Screening Yields a Remarkable Class of Protein Phosphatase Methylesterase-1 Inhibitors. *Proc. Natl. Acad. Sci. U.S.A* **2011**, *108*, 6811–6816.

(23) Berlin, J. M.; Fu, G. C. Enantioselective nucleophilic catalysis: the synthesis of aza-beta-lactams through [2 + 2] cycloadditions of ketenes with azo compounds. *Angew. Chem., Int. Ed. Engl.* **2008**, *47*, 7048–7050.

(24) Leung, D.; Hardouin, C.; Boger, D. L.; Cravatt, B. F. Discovering potent and selective reversible inhibitors of enzymes in complex proteomes. *Nature Biotechnol.* **2003**, *21*, 687–691.

(25) Adibekian, A.; Martin, B. R.; Wang, C.; Hsu, K. L.; Bachovchin, D. A.; Niessen, S.; Hoover, H.; Cravatt, B. F. Click-generated triazole ureas as ultrapotent in vivo-active serine hydrolase inhibitors. *Nature Chem. Biol.* **2011**, doi: 10.1038/nchembio.579.

(26) Powers, J. C.; Asgian, J. L.; Ekici, O. D.; James, K. E. Irreversible inhibitors of serine, cysteine, and threonine proteases. *Chem. Rev.* **2002**, *102*, 4639–4750.

(27) Weerapana, E.; Simon, G. M.; Cravatt, B. F. Disparate proteome reactivity profiles of carbon electrophiles. *Nature Chem. Biol.* **2008**, *4*, 405–407.

(28) Li, W.; Blankman, J. L.; Cravatt, B. F. A functional proteomic strategy to discover inhibitors for uncharacterized hydrolases. *J. Am. Chem. Soc.* **2007**, *129*, 9594–9595.

(29) Hoover, H. S.; Blankman, J. L.; Niessen, S.; Cravatt, B. F. Selectivity of inhibitors of endocannabinoid biosynthesis evaluated by activity-based protein profiling. *Bioorg. Med. Chem. Lett.* **2008**, *18*, 5838–5841.

(30) Kidd, D.; Liu, Y.; Cravatt, B. F. Profiling serine hydrolase activities in complex proteomes. *Biochemistry* **2001**, *40*, 4005–4015.

(31) Liu, Y.; Patricelli, M. P.; Cravatt, B. F. Activity-based protein profiling: the serine hydrolases. *Proc. Natl. Acad. Sci. U.S.A.* **1999**, *96*, 14694–14699.

(32) Patricelli, M. P.; Giang, D. K.; Stamp, L. M.; Burbaum, J. J. Direct visualization of serine hydrolase activities in complex proteome using fluorescent active site-directed probes. *Proteomics* **2001**, *1*, 1067–1071.

(33) Adam, G. C.; Sorensen, E. J.; Cravatt, B. F. Proteomic profiling of mechanistically distinct enzyme classes using a common chemotype. *Nature Biotechnol.* **2002**, *20*, 805–809.

(34) Jessani, N.; Niessen, S.; Wei, B. Q.; Nicolau, M.; Humphrey, M.; Ji, Y.; Han, W.; Noh, D. Y.; Yates, J. R., III; Jeffrey, S. S.; Cravatt, B. F. A streamlined platform for high-content functional proteomics of primary human specimens. *Nature Methods* **2005**, *2*, 691–697.

(35) Washburn, M. P.; Wolters, D.; Yates, J. R., III. Large-scale analysis of the yeast proteome by multidimensional protein identification technology. *Nature Biotechnol.* **2001**, *19*, 242–247.

(36) Eng, J.; McCormack, A. L.; Yates, J. R. An approach to correlate MS/MS data to amino acid sequences in a protein database. *J. Am. Soc. Mass Spectrom.* **1994**, *5*, 976–989.

(37) Keller, A.; Nesvizhskii, A. I.; Kolker, E.; Aebersold, R. Empirical statistical model to estimate the accuracy of peptide identifications made by MS/MS and database search. *Anal. Chem.* **2002**, *74*, 5383–5392.

(38) Tabb, D. L.; McDonald, W. H.; Yates, J. R. DTASelect and Contrast: tools for assembling and comparing protein identifications from shotgun proteomics. *J. Proteome Res.* **2002**, *1*, 21–26.

(39) Weerapana, E.; Wang, C.; Simon, G. M.; Richter, F.; Khare, S.; Dillon, M. B.; Bachovchin, D. A.; Mowen, K.; Baker, D.; Cravatt, B. F. Quantitative reactivity profiling predicts functional cysteines in proteomes. *Nature* **2010**, *468*, 790–795.